Biochimica et Biophysica Acta 1858 (2017) 249–258

Contents lists available at ScienceDirect

Biochimica et Biophysica Acta

journal homepage: www.elsevier.com/locate/bbabio

Reevaluating the mechanism of excitation energy regulation in iron-starved cyanobacteria

Hui-Yuan S. Chen [a], Michelle Liberton [b], Himadri B. Pakrasi [a,b], Dariusz M. Niedzwiedzki [c,*]

[a] Department of Energy, Environmental, and Chemical Engineering, Washington University in St. Louis, St. Louis, MO 63130, USA
[b] Department of Biology, Washington University in St. Louis, St. Louis, MO 63130, USA
[c] Photosynthetic Antenna Research Center, Washington University in St. Louis, St. Louis, MO 63130, USA

ARTICLE INFO

Article history:
Received 14 October 2016
Received in revised form 20 December 2016
Accepted 6 January 2017
Available online 8 January 2017

Keywords:
IsiA
Carotenoids
Excitation quenching
Cyanobacteria
Transient absorption
Chlorophyll

ABSTRACT

This paper presents spectroscopic investigations of IsiA, a chlorophyll *a*-binding membrane protein produced by cyanobacteria grown in iron-deficient environments. IsiA, if associated with photosystem I, supports photosystem I in light harvesting by efficiently transferring excitation energy. However, if separated from photosystem I, IsiA exhibits considerable excitation quenching observed as a substantial reduction of protein-bound chlorophyll *a* fluorescence lifetime. Previous spectroscopic studies suggested that carotenoids are involved in excitation energy dissipation and in addition play a second role in this antenna complex by supporting chlorophyll *a* in light harvesting by absorbing in the spectral range inaccessible for chlorophyll *a* and transferring excitation to chlorophylls. However, this investigation does not support these proposed roles of carotenoids in this light harvesting protein. This study shows that carotenoids do not transfer excitation energy to chlorophyll *a*. In addition, our investigations do not support the hypothesis that carotenoids are quenchers of the excited state of chlorophyll *a* in this protein complex. We propose that quenching of chlorophyll *a* fluorescence in IsiA is maintained by pigment-protein interaction via electron transfer from an excited chlorophyll *a* to a cysteine residue, an excitation quenching mechanism that was recently proposed to regulate the light harvesting capabilities of the bacteriochlorophyll *a*-containing Fenna-Mathews-Olson protein from green sulfur bacteria.

1. Introduction

Cyanobacteria are oxygenic photosynthetic organisms that are responsible for a significant portion of global biomass production. They are genetically and morphologically diverse and are found in various environments across a wide range of altitudes and latitudes [1]. Cyanobacteria have survived many geological and climatic changes on Earth during the past ~3.5 billion years, and have evolved to overcome severe environmental conditions, such as nutrient deficiencies [2]. Iron deficiency is a common nutrient-deficient condition in cyanobacterial habitats. Although iron is one of the most abundant elements on Earth, it is usually found in the form of insoluble ferric oxides [3,4]. Cyanobacteria need significant amounts of ferric iron (Fe^{3+}) for assembly of iron-sulfur complexes, which are necessary for maintaining light-dependent photochemical reactions in protein complexes like photosystem I (PSI) [5]. If the surrounding environment lacks iron, cyanobacteria cannot produce sufficient levels of PSI or other essential iron-sulfur proteins, which may have lethal consequences.

IsiA is a chlorophyll *a* (Chl *a*)-binding protein produced by cyanobacteria living in iron-deficient conditions [6]. Given that iron limitation is common in natural environments, under such conditions the IsiA protein is produced and associated with PSI [7–9], where it participates in the process of light harvesting. IsiA is a 36 kDa membrane protein with high protein sequence homology to CP43, a core light-harvesting antenna protein of photosystem II (PSII) [7]. A major difference between these proteins is their pigment content. While CP43 binds 13 Chl *a* and three molecules of carotenoid β-carotene, IsiA contains between 13 and 16 Chl *a* and four carotenoids: three β-carotenes and one echinenone [10,11]. A high-resolution crystal structure of the IsiA protein is not available, but top view images obtained by electron microscopy analysis of single particles of PSI-IsiA supercomplexes showed that the PSI trimer is surrounded by 18 IsiA subunits forming a $(PSI)_3(IsiA)_{18}$ supercomplex [8]. This ring-shaped supercomplex is a preferred formation adapted by $(PSI)_x(IsiA)_y$ supercomplexes [12].

Since the identification of the IsiA protein in the 1980s [6], several hypotheses have been proposed to explain its biological function. IsiA is highly homologous with CP43, but is produced when the cyanobacterial cells are grown in iron-deficient environments where adequate quantities of PSI cannot be assembled [13]. It was suggested that the protein is synthesized to compensate for the loss of PSI and maintain light harvesting capacity. From this perspective, the IsiA

* Corresponding author at: Washington University, One Brookings Drive, St. Louis, MO 63130, USA.
E-mail address: niedzwiedzki@wustl.edu (D.M. Niedzwiedzki).

http://dx.doi.org/10.1016/j.bbabio.2017.01.001
0005-2728/

rings formed around PSI may act as huge light harvesting antennas, similar to phycobilisomes associated with PSII [14]. Due to a high mobility of IsiA in thylakoid membranes and a large pigment capacity, a function in Chl *a* storage has been also proposed [15].

Studies using time-resolved optical spectroscopies [11,16] suggested that in PSI-IsiA supercomplexes, IsiA very efficiently transfers the excitation energy of absorbed light to PSI. However, antenna proteins that are separated from PSI and freely float in the thylakoid membrane show a protective, dissipative mechanism that mitigates potential photo-oxidative damage. Excitation quenching has been clearly observed as a substantial shortening of the excited state lifetime of Chl *a* [10]. Further investigations proposed that a quenching mechanism based on non-photochemical quenching was present at the level of the protein monomer and maintained by carotenoids. It was argued that one of the carotenoids, preferentially echinenone, quenches the singlet excited state of Chl *a* via direct energy transfer from the Chl *a* Q_y state to the carotenoid S_1 state [17,18].

Efficient quenching of the Chl *a* excited state via the carotenoid S_1 state can compete with the intrinsic decay of the carotenoid S_1. If the pool of carotenoids excited to their S_1 state via chlorophyll-to-carotenoid energy transfer is populated faster than the intrinsic decay of the S_1 state, the state can be detected by time-resolved absorption spectroscopy by recording the $S_1 \rightarrow S_n$ excited state absorption band. This provides direct evidence of carotenoid involvement in the quenching process. Recently, this spectroscopic method directly demonstrated the involvement of a carotenoid in Chl *a* quenching in another class of cyanobacterial proteins called High-Light Inducible Proteins [19,20]. No such spectral signature of the carotenoid excited S_1 state has ever been experimentally observed for IsiA. An explanation that has been provided was based on the hypothesis that the populating rate of the quencher (echinenone in the S_1 state) is not fast enough to compensate for a subsequent, immediate decay of its excited state. The excited carotenoid will be only a "virtual" element in the excitation decay pathway. Thus carotenoid involvement was simply anticipated and built into kinetic models of the Chl *a* excitation decay path [17,18].

Furthermore, the absorption spectrum of the IsiA sample used in the previous studies [17,18] showed a maximum of absorption of the Chl *a* Q_y band shifted to 675 nm, which according to other spectroscopic studies is more characteristic of the IsiA-PSI supercomplex [11,16,21,22]. This is strongly suggestive of a sample that could be substantially contaminated by PSI or to some extent contains a mixture of IsiA and IsiA-PSI supercomplexes. Because the effect of the quenching of Chl *a* fluorescence in the IsiA protein could be undermined by hypothetically possible IsiA-to-PSI energy transfer, this questions the conclusions of the previous studies.

The work presented here strongly suggest that carotenoids do not play a role in the energetics of this pigment protein complex, either as quenchers or supporters of Chl *a*. The results of this study strongly suggest that the quenching mechanism is merely governed by Chl *a*-protein interactions via electron transfer from an excited Chl *a* to a cysteine residue. Such a novel energy-quenching mechanism was very recently proposed to regulate the light harvesting capabilities of the bacteriochlorophyll *a*-containing Fenna-Mathews-Olson (FMO) protein from green sulfur bacteria [23]. However, the current study suggests that this mechanism could be more broadly utilized by photosynthetic organisms than initially anticipated.

2. Materials and methods

2.1. Strain growth and thylakoid membrane preparation

The IsiA-His strain of *Synechocystis* sp. PCC 6803 was constructed by oligonucleotide-directed mutagenesis to introduce six histidyl codons at the carboxy terminus of *isiA*. IsiA-His cells were grown phototrophically in BG11 medium containing kanamycin at 30 °C. The liquid cultures were shaken in Erlenmeyer flasks at 60 rpm with illumination of 30 μmol photons m^{-2} s^{-1}. After 5 days of growth, cells were washed with YBG11-Fe [24] medium three times, and inoculated into 1 L YBG11-Fe_3 medium. After about 2 weeks, the cells were then harvested and broken by bead-beating as described previously [25]. Thylakoid membranes were resuspended in Buffer A (50 mM HEPES-NaOH [pH 7.8], 10 mM $MgCl_2$, 5 mM $CaCl_2$, 25% glycerol). Membranes were solubilized by addition of β-D-dodecyl maltoside (DDM) to a final concentration of 1%. After incubation on ice in dark for 30 min, the solubilized membranes were separated from the insoluble material by centrifugation at gradually increasing speed from 120 ×*g* to 27,000 ×*g* at 4 °C for 20 min. The solubilized membranes were then stored at −80 °C for future use.

2.2. IsiA protein purification

The IsiA and PSI-IsiA complexes were purified using nickel affinity chromatography [26] with some modifications. Ni-NTA slurry was precharged with 50 mM nickel sulfate overnight and loaded into an open column. The resin was washed with 25 column volumes of water, and then twice with 5 column volumes of Buffer A plus 0.04% DDM and 5 mM histidine to remove ethanol and nickel sulfate. After continuous mixing of the washed resin with the previously prepared solubilized membranes at 4 °C for 2 h, the flow through material was collected. The resin was then washed with 1 column volume Buffer A plus 0.04% DDM and 5 mM histidine. To remove all other unbound proteins, 12 column volumes of Buffer A plus 0.04% DDM was used to wash the resin. The eluents were collected and absorption was measured using a DW2000 spectrophotometer (OLIS, USA) to verify that any residual unbound chlorophyll-containing proteins had been washed from the column. The target proteins, PSI-IsiA supercomplexes and IsiA proteins, were eluted with 6 column volumes of buffer A plus 0.04% DDM and 100 mM histidine. To concentrate the proteins, 80% (v/v) PEG8000 in 30 mM HEPES-NaOH (pH 7.8) was added into the elution, and the proteins were precipitated by centrifugation at 31,000 ×*g* for 15 min. The precipitated proteins were resuspended in Buffer A plus 0.04% DDM.

Sucrose gradient ultracentrifugation was used to obtain highly purified IsiA aggregates that do not contain PSI. The PEG-concentrated protein sample was diluted in glycerol-free Buffer A plus 0.04% DDM and then loaded on the top of a 10–35% sucrose gradient in glycerol-free Buffer A plus 0.04% DDM. Centrifugation was performed using a swinging bucket type Beckman-Coulter SW41 rotor at 4 °C and relative centrifugal force of 186,000 ×*g*. After 18 h of ultracentrifugation, green bands were collected. The first green band from the top of the gradient was determined spectroscopically to contain IsiA only, and was stored at −80 °C until future use.

2.3. SDS-PAGE and immunoblot analysis

SDS-PAGE was performed by loading the isolated PSI-IsiA supercomplexes and IsiA protein samples (adjusted to Chl *a* mass weight of 0.75 μg) on a 12.5% acrylamide resolving gel. After transfer of the proteins onto a PVDF membrane, IsiA and PsaA were detected by using specific antisera. Bands were visualized using chemiluminescence reagents (EMD Millipore, Billerica, MA, USA) with an ImageQuant LAS-4000 imager (GE Healthcare).

2.4. Spectroscopic techniques

For all low-temperature spectroscopic measurements, the IsiA or IsiA-PSI samples were mixed with glycerol in a 1:1 (v/v) ratio, placed in 1 cm square plastic cuvettes and frozen in a VNF-100 liquid nitrogen cryostat (Janis, USA). Steady-state absorption measurements were performed using a Shimadzu UV-1800 spectrophotometer. Fluorescence and fluorescence-excitation spectra were recorded at room temperature using a Horiba-Spex Nanolog fluorometer. The spectra were

recorded at 90° to excitation and corrected for the instrument spectral response. The excitation and detection bandwidths were 2–4 nm. To avoid front-face and inner-filter effects, the samples were adjusted to an absorbance ≤0.1 at the excitation and emission wavelengths.

Time-resolved fluorescence (TRF) experiments were carried out using two different setups. The Hamamatsu universal streak camera setup described in detail previously [27] was used to obtain multi-wavelength decay profiles. The frequency of the excitation pulses was set to 8 MHz, corresponding to ~120 ns between subsequent pulses. The excitation beam was set to 630 nm, with photon intensity of ~10^{10} photons/cm^2 per pulse, depolarized and focused on the sample in a circular spot of ~1 mm diameter. The sample absorbance was adjusted to ~0.1 at the Q_y band of Chl *a* in a 1 cm cuvette. The emission was measured at a right angle to the excitation beam. To minimize the detection of scattered light from the excitation beam a long-pass 665 nm filter was placed at the entrance slit of the spectrograph. The integrity of the samples was examined by observing the photon counts in real-time over the time course of the experiment. These were constant, which indicated the absence of sample photodegradation. Single wavelength decay measurements were performed using a standalone Simple-Tau 130 time-correlated single photon counting (TCSPC) setup from Becker&Hickl (Germany) coupled to an ultrafast laser system (Spectra-Physics, USA) described in detail previously [28]. The IsiA complexes were resuspended to an absorbance of ≤0.1 at the Chl *a* Q_y band and the emission signal was recorded at a right angle with respect to the excitation beam.

Transient absorption (TA) measurements of the IsiA protein were performed using a Helios TA spectrometer (UltrafastSystems LCC, Sarasota, FL, USA) coupled to a Spectra-Physics femtosecond laser system described previously in detail [29]. The white light continuum probe was generated by a 3 mm thick CaF_2 plate. The pump beam with energy set to 0.1 μJ (670 nm, Chl *a*) or 0.2 μJ (505 nm, carotenoids) was focused to a spot size of 1 mm in diameter, corresponding to intensity of ~4–6 × 10^{13} photons/cm^2. The sample was adjusted to an absorbance of 0.4 at the Chl *a* Q_y band (1 cm path length).

2.5. Data analysis and fitting

Dispersion in TA datasets was corrected using the Surface Xplorer, software provided by Ultrafast Systems, by applying a dispersion correction. Directed kinetic modeling, referred to as target analysis, of the TRF and TA results was performed using CarpetView, a data viewing and analysis software for ultrafast spectroscopy measurements (Light Conversion Ltd., Vilnius, Lithuania). The fitting procedures used the kinetic models with anticipated realistic decay pathways following excitation of a carotenoid or Chl *a*. If the underlying assumptions are correct, targeted kinetic analysis separates spectral components such as excited state absorption (ESA) of the specific excited states of molecules, etc. The results are commonly abbreviated as SADS - Species Associated Decay Spectra [30]. We have adapted this nomenclature to the fitting results of both TA and TRF datasets. For fitting purposes, the instrument response function (IRF) was assumed to have a Gaussian-like shape with the full width at half maximum (FWHM) of ~200 fs for TA and 70 ps, 180 ps and 320 ps for TRF in 1, 5 and 10 ns time windows, respectively. This parameter was fixed in the fitting procedures.

3. Results and discussion

3.1. Characterization and steady-state spectroscopy of the PSI-IsiA and IsiA complexes

The protein bands obtained after the sucrose gradient ultracentrifugation, the final step of IsiA protein purification, are shown in Fig. 1A. The top green band with the lowest mass density was targeted as a candidate for IsiA-only complexes. Further analysis of this band by western blotting (Fig. 1B) confirmed the absence of the PSI core subunit PsaA. Furthermore, the strong band shown on the blot probed by the IsiA antibody showed the presence of IsiA, thus confirming that it contained pure IsiA-only complexes. On the other hand, the PSI-IsiA sample contained both PSI and IsiA as expected. Room temperature absorption spectra of the IsiA, PSI and PSI-IsiA samples are provided in Fig. 1C. This analysis showed very distinctive differences in the Q_y band of Chl *a*. The Q_y absorption band appears at 670 nm in the IsiA sample but is shifted to longer wavelengths for the PSI complex (679 nm) and for the PSI-IsiA supercomplex (674 nm). Fig. 1D shows absorption spectra taken at 77 K. As visualized by the green dashed line, the absorption of the PSI-IsiA supercomplex was very adequately mimicked by the weighted sum of the individual spectra of the IsiA and PSI complexes.

The good agreement of the spectral shapes of the native and reconstructed PSI-IsiA spectra indicated that there was no excitonic coupling between Chls from IsiA and PSI proteins, as that would affect the shape of the Q_y band. The near-identical spectral lines of native and mimicked absorption spectra suggest that there are no additional pigments (carotenoid, Chl *a*) that are weakly bound in the IsiA and PSI interface and that could be lost during separation of the supercomplex into individual complexes during detergent treatment.

Past studies reported that carotenoids transfer excitation energy to Chl *a* with an overall efficiency of ~25%, suggesting that those pigments also supplement Chl *a* in light harvesting in the IsiA complex [17]. However, this hypothesis was based on kinetic modeling of transient absorption data and additional support was not provided [17]. Our fluorescence studies (Fig. 2) clearly showed that carotenoids are essentially not involved in supporting Chl *a* in light harvesting. The fluorescence excitation (Exc) spectrum did not show any evidence of a carotenoid absorption band, as seen in the absorptance (1-T, where T is transmittance) spectrum. Assuming 100% energy transfer within Q_y (profiles are normalized there), carotenoid-to-Chl *a* energy transfer efficiency was essentially zero as there was no contribution in the Exc profile of IsiA that could be assigned to carotenoids (between 450 and 550 nm). There are no available prior results of Chl *a* fluorescence excitation of the IsiA protein for comparison. The profile recorded for a highly homologous protein CP43 shows that energy transfer from carotenoids to Chl *a* is very small in that protein [31], which is consistent with the results obtained for IsiA in this study.

3.2. Time-resolved fluorescence of PSI-IsiA and IsiA complexes

Fig. 3 shows TRF results from PSI-IsiA and IsiA complexes recorded at RT and at 77 K. The two-dimensional pseudo-color profiles of TRF of the samples are given in panels A, C and E, and the corresponding global analyses of the datasets are shown in panels B, D and F. Cryogenic temperature essentially had no effect on IsiA-to-PSI energy transfer. As demonstrated in Fig. 3A, excitations populated initially on IsiA were promptly transferred to PSI. Target analysis of TRF data showed that transfer time could not be precisely defined, as it was shorter than the streak camera temporal resolution in this time window (FWHM of IRF is ~70 ps in a 1 ns time window). The spectral characteristics of other kinetic components strongly suggest that those are associated with excitation equilibration and followed excitation decay within the Chl *a* array in PSI.

Global fitting of the RT TRF data of separate IsiA samples addressed two kinetic components with lifetimes of 300 ps and 1.7 ns. The fitting protocol assumed that both fractions were independently populated and decayed without interacting with each other. The spectral profiles of SADS showed identical lineshapes. These lifetimes are comparable to those observed in the fluorescence decay of quenched IsiA aggregates in which a short kinetic component lifetime of ~200 ps dominates [10]. Interestingly, a substantial alteration of fluorescence lifetime distribution occurs if the IsiA protein is cooled to 77 K. Fitting results (Fig. 3F) demonstrated that the lifetimes substantially elongate to 1.9 ns and 6.8 ns but the spectral lineshapes of both SADS remain identical, though the fluorescence band is narrower and slightly red-shifted at 77 K. To

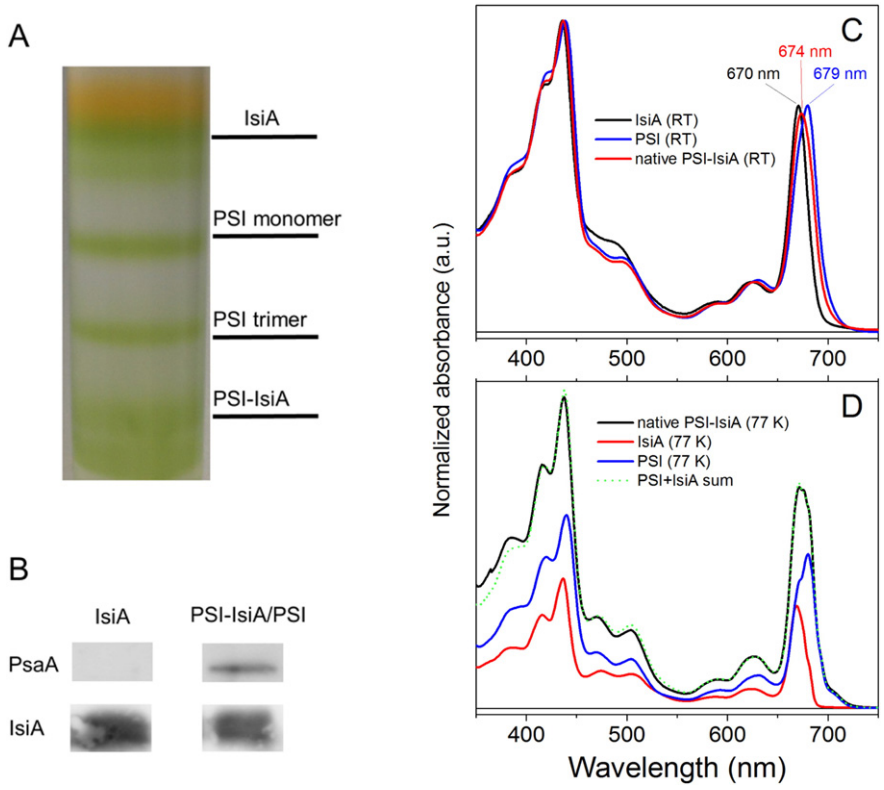

Fig. 1. Purification and basic spectroscopic characterization of IsiA and PSI-IsiA. (A) Protein bands obtained from sucrose gradient ultracentrifugation, (B) PSI-IsiA complexes purified by nickel affinity chromatography and the IsiA band from ultracentrifugation probed by immunoblotting, (C) Room temperature and (D) 77 K absorption spectra of PSI-IsiA complexes and individual IsiA and PSI (with absorptions adjusted to relative contributions in the PSI-IsiA spectrum).

assure that elongation of fluorescence lifetime is truly a temperature dependent effect and is not simply due to the presence of glycerol in the buffer, we have compared dynamics of Chl *a* fluorescence decay of the IsiA protein diluted only in the buffer and in the buffer-glycerol mixture, measured at RT. These results are given in supplementary information (Fig. S1) and demonstrate that adding glycerol has a negligible impact on IsiA fluorescence dynamics. Fig. 3G shows the comparison of representative kinetic traces of fluorescence decay for IsiA-containing samples under different conditions: IsiA coupled with PSI at 77 K (cyan line), and IsiA aggregates at RT (blue line) and at 77 K (red line). Lifetime shortening of IsiA-bound Chl *a* fluorescence upon coupling to PSI is understandable and is associated with IsiA-PSI energy transfer; however, the substantial elongation of the Chl *a* excited state lifetime in IsiA aggregates after cooling to cryogenic temperature is not easy to interpret and merits further investigation.

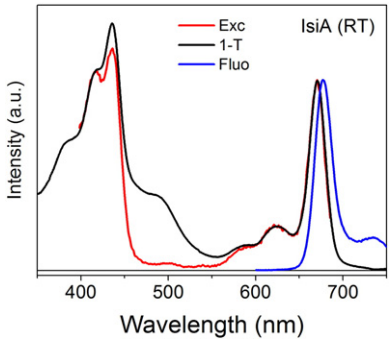

Fig. 2. Fluorescence excitation (Exc), emission (Fluo) and absorptance (1-T, T-transmittance) spectral profiles of the IsiA complex at room temperature.

3.3. Time-resolved absorption spectroscopy of the IsiA complex

The strong dependence of the lifetime of excited Chl *a* in IsiA samples on temperature, as demonstrated in the time-resolved fluorescence studies, questions the idea that carotenoids are responsible for Chl *a* quenching. Previous studies on carotenoid-mediated Chl *a* quenching in another cyanobacterial chlorophyll protein from a family of High-Light Inducible Proteins (Hlips) clearly demonstrated that the quenching ability of the carotenoid is essentially not affected by low temperature [19] and elongation of the effective lifetime of the quenched Chl *a* is not expected. In addition, at cryogenic temperature, the carotenoid reveals a very prominent electrochromic response to excited Chl *a*. An electrochromic response of carotenoid that interacts with either Chl *a* or BChls is not unusual; on the contrary, it is typically observed in many other photosynthetic proteins like PCP from dinoflagellates [32] or LH2 and LH1 light harvesting complexes from purple bacteria [33–36], particularly at cryogenic temperature. In those proteins, carotenoids actually play a role as either singlet energy donors or (B)Chls triplet quenchers. Both of these roles require that carotenoid and (B)Chl molecules are in close proximity, and thus in both cases carotenoid absorption should be similarly affected by the change in the surrounding electric field induced by the (B)Chl excited state. We applied time-resolved absorption to test if the electrochromic effect on carotenoid absorption is also observed in IsiA. A negative result would indicate that carotenoids are likely not responsible for the Chl *a* quenching that is observed at RT, as the lack of electrochromic response to the excited Chl *a* would indicate that both pigments are not at a distance that allows energy transfer between them.

The results obtained for IsiA measured at 77 K are given in Fig. 4. In order to test all possible outcomes, the sample was excited at wavelengths corresponding to absorption bands of all bound pigments: β-carotene (at 505 nm), echinenone (at 535 nm) and Chl *a* (Q_y band, at

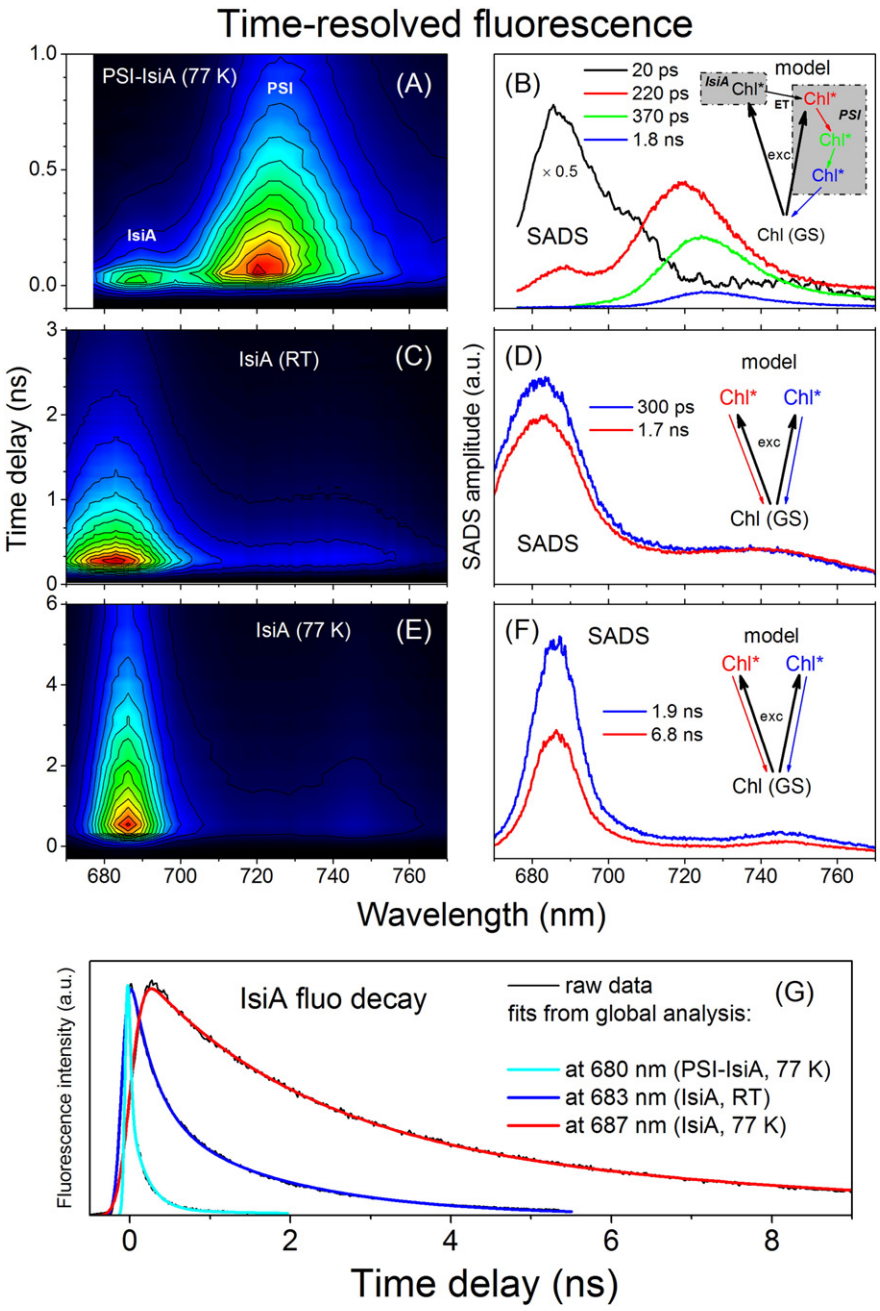

Fig. 3. Time-resolved fluorescence of PSI-IsiA and IsiA complexes at RT and at 77 K. (A, C, E) Two dimensional, pseudo-color fluorescence decay profiles of PSI-IsiA at 77 K, IsiA at RT and at 77 K, respectively. (B, D, F) Global analysis results of TRF datasets (SADS) with application of anticipated kinetic schemes of the excitation decay. The models are provided as insets. The legends contain effective lifetimes of spectro-kinetic components obtained from the analysis. (G) Representative traces of the IsiA fluorescence decay extracted for the datasets along with corresponding fits obtained from global analysis. exc - excitation, GS - ground state, ET - energy transfer, Chl – chlorophyll *a*, SADS – species associated decay spectra.

670 nm). Representative transient absorption spectra obtained after excitation of the carotenoid bands are given in Fig. 4A and B. The spectra consist mostly of features associated with bleaching of the ground state absorption of the carotenoid (the negative region mirroring expected steady-state absorption of the carotenoid in IsiA) and associated positive excited state absorption, $S_1 \rightarrow S_n$, transient band. For β-carotene, this band peaks at 680 nm, for echinenone at 600 nm. Previous TA study of this protein suggested that instantaneous and prominent bleaching of the Q_y band of Chl *a* upon excitation of the carotenoid band was a clear indication of carotenoid to Chl *a* energy transfer presumably via S_2 state. For echinenone, the quantum efficiency of the energy transfer process was estimated to be ~40% [17]. However, such interpretation of the TA results does not agree with fluorescence excitation that shows that carotenoid-to-Chl *a* energy transfer is negligible. It is clear that the signal with apparent Chl *a* signatures must come from direct excitation of Chl *a* to a vibronic overtone of the Q_y band. To further elaborate and prove that it is possible we performed TA study of the Chl *a*-β-carotene mixture dissolved in *n*-hexane. The mixture closely mimicked absorption spectrum of the IsiA protein sample. In the mixture, energy transfer between pigments is negligible and upon excitation of the carotenoid band any signal associated with Chl *a* should derive from its direct excitation. These results, shown in Fig. S2, also support the idea of self-origin of Chl *a* signal in the IsiA sample upon carotenoid band excitation.

The TA data were fitted with anticipated models of the excitation decay path, and the resulting spectro-kinetic profiles (SADS) are given in Fig. 4C and D. To simplify fitting, the spectral range comprising the Chl *a* Q_y band was not included. The SADS lifetimes of 10.5 and 6.6 ps

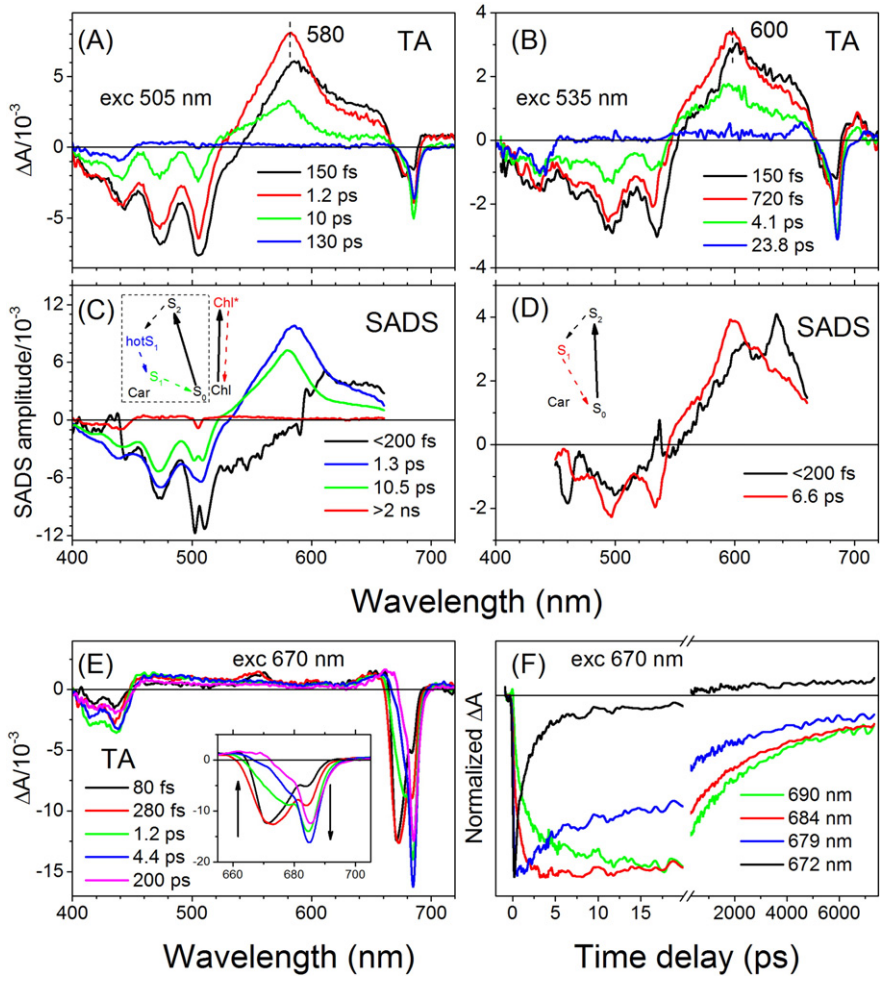

Fig. 4. Time-resolved absorption of the IsiA complex at 77 K. (A, B) Representative TA spectra after selective excitation of the carotenoid absorption band: β-carotene (excitation at 505 nm) and echinenone (excitation at 535 nm). (C, D) Species associated difference spectra (SADS) resulting from global analysis of the TA datasets with application of the kinetic models provided in the graph inserts. (E) Representative TA spectra taken after excitation at the blue edge of the Chl *a* Q_y absorption band at 670 nm. (F) Representative kinetic traces of rise and decay of the Q_y band probed at multiple wavelengths.

associated with decay of the S_1 state indicate that both carotenoid pigments perform essentially as in frozen solvent (for echinenone, 3′-hydroxyechinenone was used as a benchmark) [37,38], and binding to the protein does not induce any geometrical distortions, as that typically would affect those lifetimes.

Representative spectra of 77 K transient absorption of IsiA upon excitation of the Q_y band of Chl *a* are given in Fig. 4E. In early delay times the spectra indicate rapid energy transfer within two different spectral forms of Chl *a*, as indicated by the split Q_y band (see insert). This intermolecular Chl *a*-Chl *a* energy flow is also well indicated in the kinetic traces provided in Fig. 4F. More importantly, there is no signature of a carotenoid electrochromic response, either in β-carotene or echinenone. A bump appearing between 540 and 580 nm within the first 200 fs is also visible in blank buffer (not shown), indicating it is clearly associated with solvent response to the excitation.

More insight into the kinetic characteristics of Chl *a* in IsiA at 77 K is given in Fig. 5. Fig. 5A shows that rapid decay of the Chl *a* bleaching band at 671 nm is coupled with the rise of the bleaching of the band at 684 nm. The time constant of 1.3 ps obtained from fitting of the decay trace at 671 nm, matches very well with the rise constant of 1.1 ps observed in the 684 nm trace. This strongly indicates that none of the excitation initially localized on Chls absorbing at 670 nm is lost, but that it is essentially instantaneously passed on to low-energy Chls. This demonstrates that the Chl *a* array in this protein is very well optimized to minimize any potential loss of excitation during migration within IsiA.

On the other hand, recovery of the bleaching of the 684 nm Q_y band should temporarily show the same characteristics as the time-resolved fluorescence data because most likely the same pool of Chls is probed in both techniques. However, it should be noted that since an amplified laser excitation beam is used in transient absorption measurements, it is possible that multiple excitations are simultaneously populated within the Chl *a* exciton manifold and singlet-singlet annihilation will be unavoidable. Because the extent of this process is laser intensity dependent, it could be easily spotted by comparing the kinetic traces recorded upon vastly different excitation laser intensities. This is given in Fig. 5B, which shows the recovery of the bleaching of the Chl *a* Q_y band at 684 nm for two substantially different excitation fluxes. Because both traces, normalized at amplitudes, do not overlap, and the kinetic trace obtained at higher laser intensity initially decays faster, involvement of singlet-singlet annihilation is apparent. Consequently, an appropriate fitting model should account for an annihilation process. If it is assumed that the time of convoluting the Chl *a* transient signal (exciton generation) is negligible compared to the following decay, the 684 nm kinetic trace could be fitted according to the following equation that was adopted from [39]:

$$\Delta A(t) = \frac{\Delta A_1 e^{-kt}}{1 + \Delta A_1 \gamma_{s-s} k^{-1}\left(1 - e^{-kt}\right)} + \Delta A_2 e^{-kt} + \Delta A_2 e^{-k_1 t} \quad (1)$$

Where $\gamma_{S\text{-}S}$ is the time-independent annihilation rate and k and k_1 are decay rates of Chl fractions that are not affected by singlet-singlet

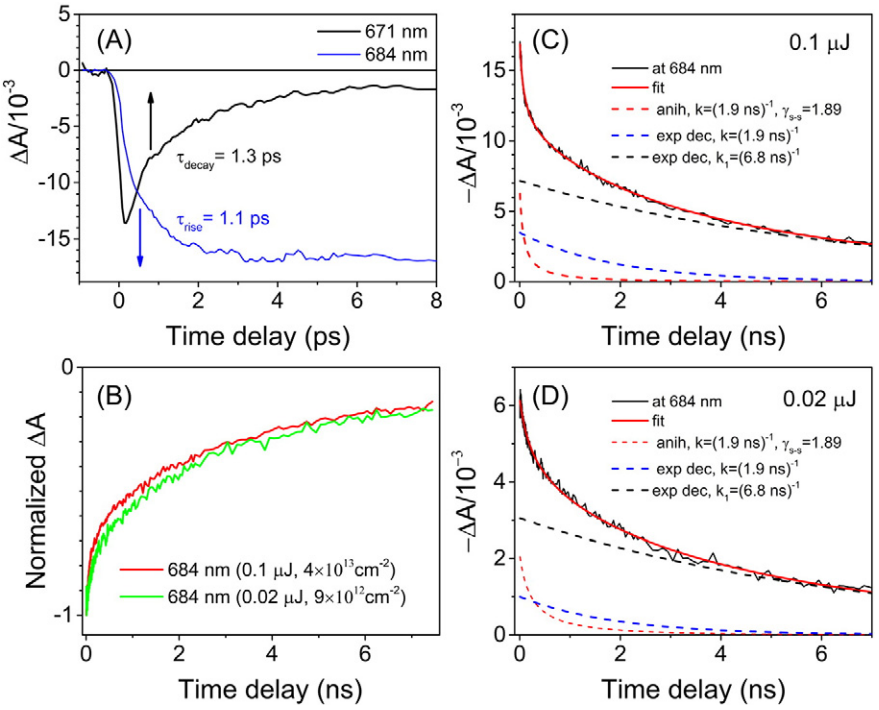

Fig. 5. Temporal characteristics of recovery of the Chl *a* Q_y band of IsiA at 77 K. (A) Rise and decay of two Q_y sub-bands resolved by TA at 77 K. (B) Dependence of recovery dynamics on excitation intensity. (C, D) Fitting of kinetic traces according to Eq. (1).

annihilation and should correspond to reciprocals of lifetimes obtained from time-resolved fluorescence. It was also assumed that the annihilation process would involve only the Chl *a* fraction that decays with a faster rate *k*. The results of fitting of both traces (lower and higher laser intensity) are given in Fig. 5C and D. Fitting demonstrates very good agreement with results obtained from time-resolved fluorescence.

3.4. Role of carotenoids in the IsiA protein

Previous investigations proposed that carotenoids play a dual role in the IsiA protein augmenting Chl *a* in light harvesting, and furthermore, if necessary, serving as quenchers of excited Chl *a* [17,18]. However, our work does not support these suggested roles. The Chl *a* florescence excitation study shows that none of the two carotenoid species transfers absorbed light energy to Chls. Time-resolved fluorescence experiments showed that the kinetic component (fast decay) that was previously targeted as a signal associated with the decay of quenched Chl *a* [10] substantially elongates at low temperature. This fact is difficult to explain because carotenoid-mediated quenching seems to be rather independent of temperature [19] and the lifetime of quenched Chl *a* should not be affected. Moreover, cryogenic time-resolved absorption data revealed that none of the bound carotenoids show an electrochromic response to excited Chl *a*, a feature commonly seen in light harvesting proteins in which carotenoid and (B)Chl are bound in sufficient proximity to allow energetic interaction between them.

3.5. Toward a new quenching mechanism

A clue that a novel type of quenching mechanism may be present in the IsiA protein is that, upon lowering the temperature, Chl *a* fluorescence decay substantially elongates. A similar effect is well-known for another light harvesting protein, the Fenna-Matthews-Olson (FMO) protein from green sulfur bacteria. The FMO protein, which lacks carotenoids and comprises only BChl *a* pigments, if kept in oxygenated solution displays a very short BChl *a* fluorescence lifetime of ~60 ps, which is short enough to efficiently compete with energy transfer to the reaction center (RC) in the FMO-RC complex [40–42]. However, if conditions change to reducing, the BChl *a* fluorescence lifetime mysteriously elongates to ~2 ns, close to the intrinsic decay of the excited state of monomeric BChl *a* in solution [43]. However, a substantial elongation of fluorescence lifetime can also be achieved by freezing an oxidized FMO sample to cryogenic temperature [44]. This appears to resemble the phenomenon seen for IsiA in this work. Even though the effect of reductant on BChl *a* fluorescence in the FMO protein was known for almost three decades, only very recently was its nature explained. It was demonstrated that in aerobic conditions the cysteine thiols are converted to thiyl radicals, and if those are in proximity to BChl *a*, they may quench the pigment excited state through electron transfer photochemistry [23]. It is not difficult to imagine that a similar quenching mechanism may be adopted by other photosynthetic organisms.

Cyanobacteria, which are photosynthetic organisms living in oxidizing conditions and exposed to constant iron-starvation stress, are good candidates for adopting this protective mechanism and incorporating it into a light harvesting antenna complex that is produced under challenging growth environments - IsiA. This mechanism would require the presence of cysteine in crucial places in the IsiA protein, preferentially in proximity to Chl(s) that may serve role(s) as so-called terminal emitter(s) (pass excitation to PSI) – most likely those pigments are responsible for observed fluorescence. In addition, a cysteine targeted as a quenching ligand should be quite unique, in that it must be present in IsiA but not in homologous proteins (such as CP43) that do not reveal similar Chl *a* fluorescence quenching. To test this hypothesis, we compared the IsiA and CP43 protein sequences from three cyanobacterial species and also the CP43 protein sequence from spinach, which has a high resolution crystallographic structure available (PDB ID: 3JCU) [45]. The most relevant parts of the sequence alignment are given in Fig. 6. This analysis demonstrated that cysteine is very scarce in cyanobacterial CP43 proteins, appearing only in two or three locations across the entire sequence, either on the protein side facing the membrane or not in proximity to any Chl *a*. This is consistent with the fact that CP43 does not show evidence of Chl *a* fluorescence quenching. However, the IsiA sequences show a unique cysteine that is fully conserved across the various IsiA proteins, whereas all CP43 sequences

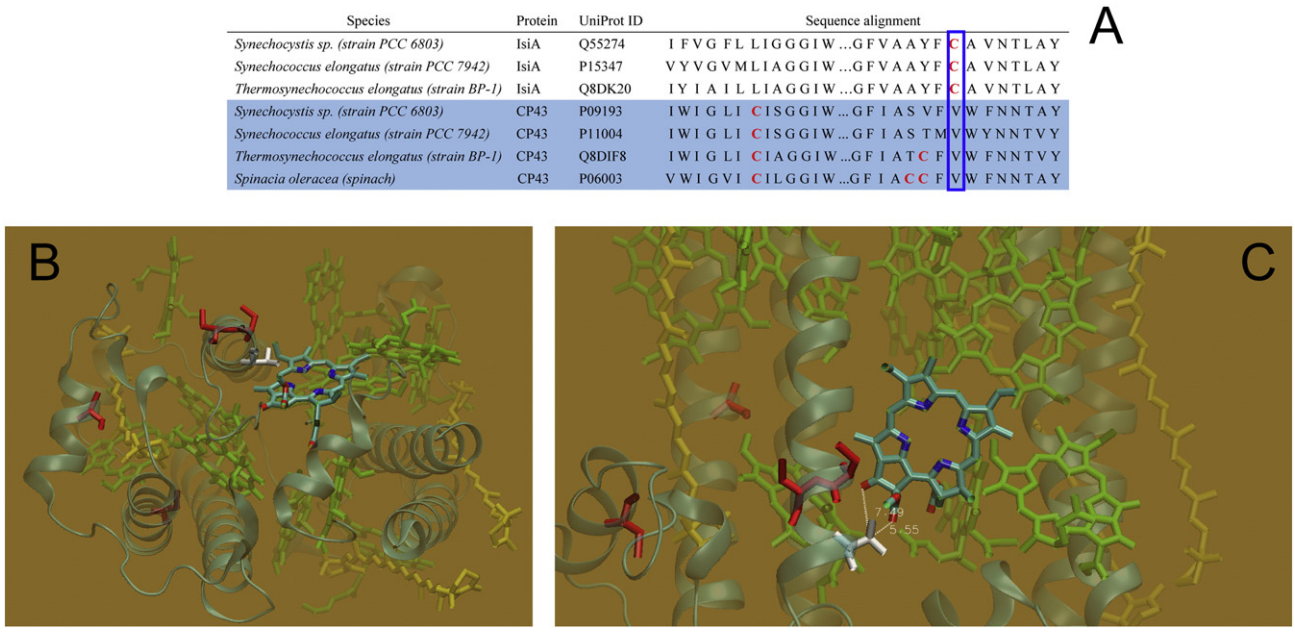

Fig. 6. Cysteines in CP43 and IsiA structures. (A) Sequence alignment of IsiA and CP43 from three cyanobacterial species, along with the sequence from spinach for which the high resolution crystal structure of CP43 is known (PDB ID: 3JCU, [45]). A simplified view of the CP43 protein molecular structure from the (B) lumenal and (C) membrane side, which in IsiA will face toward PSI. For clarity, the large extrinsic lumenal loop domain E [46] present in CP43 was removed. All possible cysteines present in various CP43 proteins across different organisms are marked in red. Valine 290, which in IsiA is replaced by cysteine and is fully conserved across multiple organisms, is marked in white.

examined have valine (Val_{290}) in this position. As shown in the simplified view of the CP43 crystal structure in Fig. 5B and C, Val_{290} is in very close proximity to a Chl *a* molecule (Chl a_{34}), according to nomenclature used in the older PSII crystal structure [47]. If replaced by cysteine, the distance between the amino acid and electron donating groups of Chl a_{34} would range between 5 and 7 Å, similar to distances observed between cysteine and BChl *a* in the FMO protein. According to the IsiA-PSI supercomplex models [22,48], Chl a_{34} is the pigment that along with other nearby Chls (Chl $a_{37, 44, 41}$) could be involved in energy transfer to PSI. Importantly, the cysteine residues that are present in the sequence of CP43 from spinach, just two places away from Val_{290}, if visualized on the structure (Fig. 6B, C) appear on the opposite side of the helix and are essentially completely shielded from any Chls. Those cysteines may not be important because they are not conserved across different photosynthetic groups, which is clearly shown in the sequence alignment (Fig. 6A). This structure-sequence analysis suggests that the IsiA protein has the capability of quenching the Chl *a* excited state through electron transfer photochemistry. Because cyanobacteria grow in aerobic conditions, the cysteine thiol in IsiA could be converted to a thiyl radical at any time and be capable of withdrawing an electron from a nearby excited Chl *a*. If this mechanism is behind the quenching of the excited state of Chl *a* in IsiA, the dynamics of protein fluorescence should be sensitive to the presence of reductant in the buffer, as is observed for FMO. Changes in the fluorescence decay dynamics of IsiA upon addition of sodium dithionite, a reductant that is typically used for FMO studies, are shown in Fig. 7.

In order to observe any changes in a more real-time fashion, a more sensitive TCSPC system was used. The fluorescence decay was measured at the maximum of the fluorescence emission spectrum (684 nm). The results show that the addition of reductant leads to an immediate change in the temporal characteristics of fluorescence decay within a minute and that the effect is essentially maximized after ~90 min. It is apparent that the short-lived component considerably elongates. It is worth noting that sodium dithionite may not be most effective reductant as it is not physiologically relevant and it is possible that other more natural, endogenous reductants (not tested here) may induce

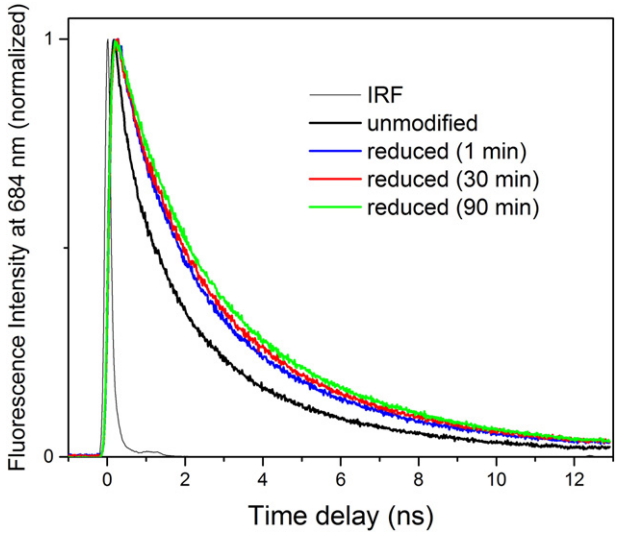

Fig. 7. Temporal changes of IsiA-bound Chl *a* fluorescence decay upon addition of sodium dithionite (to a final 10 mM concentration) to the sample buffer. Fluorescence was recorded at 684 nm at RT. IRF – instrument response function.

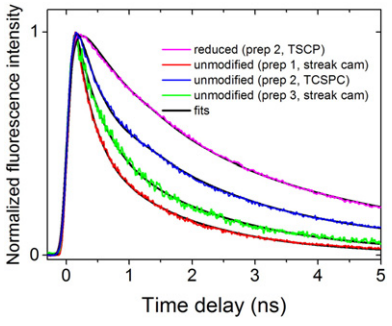

Fig. 8. Variation of dynamics of Chl *a* fluorescence decay in the unmodified IsiA protein obtained from different purification experiments (prep 1, 2, 3) and effect of adding reductant. For more details on kinetic components refer to Table 1.

Table 1
Kinetic components obtained from fitting of Chl *a* fluorescence decay traces given in Fig. 8.

Preparation	Sample[a]	τ_1 (ps)	A_1[b]	τ_2 (ns)	A_2	τ_3 (ns)	A_3	Method[c]
1	U	280	0.62	1.6	0.38	n.e.		SC
2	U	300	0.43	1.6	0.40	4.5	0.17	TCSPC
2	R	n.e.		1	0.45	4.1	0.55	TCSPC
3	U	400	0.53	2.0	0.47	n.e.		SC

[a] U – unmodified IsiA, R - reduced IsiA, n.e. - not evident.
[b] $A_1 + A_2 + A_3 = 1$.
[c] SC – streak camera, TCSPC - time-correlated single photon counting.

even more prominent effects on fluorescence decay dynamics. Nonetheless, the observed effect is a strong indication of a cysteine-dependent excitation quenching mechanism in the IsiA protein, which was only very recently found in the FMO protein.

It should be noted that the fluorescence decay trace of the unmodified IsiA seems to be different from that obtained from the experimental setup based on the streak camera (Fig. 3). Those two samples show common absorption spectra but were obtained from different purification experiments. Additional TRF experiments performed on the unmodified IsiA protein from another (third) preparation demonstrated that in each experiment, Chl *a* fluorescence kinetics of unmodified IsiA were somewhat different from each other (Fig. 8). Further analysis (Table 1) demonstrated that all decay traces share similar kinetics components, but with different weights. Such variation in amplitudes of the decay components could be associated with fluctuation in natural levels of oxidation of cysteines that may vary from preparation to preparation.

4. Conclusions

In this study we revisited the mechanism of Chl *a* excitation quenching in the IsiA protein, which is a dominant light harvesting antenna complex produced by iron-starved cyanobacteria. In contrast to previous work relying on energetic interactions of the excited Chl *a* with carotenoids present in IsiA, our study suggests that quenching of excited Chl *a* may be cysteine-dependent, similar to the quenching mechanism recently revealed in FMO, a light harvesting protein from green sulfur bacteria. We think that this finding opens many possibilities for more detailed studies of the quenching mechanism adapted by iron-starved cyanobacteria, including the influence of cysteine directed chemical modifications or cysteine directed mutations.

Transparency document

The Transparency document associated with this article can be found, in the online version.

Acknowledgements

Time-resolved spectroscopic measurements were performed in the PARC ultrafast laser facility supported as part of the Photosynthetic Antenna Research Center (PARC), an Energy Frontier Research Center funded by the U.S. Department of Energy, Office of Science, Office of Basic Energy Sciences under Award Number DE-SC 0001035. Protein isolation work was supported by Chemical Sciences, Geosciences and Biosciences Division, Office of Basic Energy Sciences, Office of Science, U.S. Department of Energy, under grant number DE-FG02-99ER20350 to HBP.

Appendix A. Supplementary data

Supplementary data to this article can be found online at http://dx.doi.org/10.1016/j.bbabio.2017.01.001.

References

[1] A. De los Rios, M. Grube, L.G. Sancho, C. Ascaso, Ultrastructural and genetic characteristics of endolithic cyanobacterial biofilms colonizing Antarctic granite rocks, FEMS Microbiol. Ecol. 59 (2007) 386–395.
[2] D.J. De Marais, Evolution. When did photosynthesis emerge on Earth? Science 289 (2000) 1703–1705.
[3] W. Stumm, J. Morgan, Aquatic Chemistry, second ed. John Wiley & Sons, New York, 1981.
[4] N. Lane, Oxygen: The Molecule That Made the World, OUP Oxford, 2002.
[5] P. Reilly, N. Nelson, Photosystem I complex, Photosynth. Res. 19 (1988) 73–84.
[6] H.B. Pakrasi, A. Goldenberg, L.A. Sherman, Membrane development in the cyanobacterium, *Anacystis nidulans*, during recovery from iron starvation, Plant Physiol. 79 (1985) 290–295.
[7] T.S. Bibby, J. Nield, J. Barber, Three-dimensional model and characterization of the iron stress-induced CP43′-photosystem I supercomplex isolated from the cyanobacterium *Synechocystis* PCC 6803, J. Biol. Chem. 276 (2001) 43246–43252.
[8] T.S. Bibby, J. Nield, J. Barber, Iron deficiency induces the formation of an antenna ring around trimeric photosystem I in cyanobacteria, Nature 412 (2001) 743–745.
[9] E.J. Boekema, A. Hifney, A.E. Yakushevska, M. Piotrowski, W. Keegstra, S. Berry, K.P. Michel, E.K. Pistorius, J. Kruip, A giant chlorophyll-protein complex induced by iron deficiency in cyanobacteria, Nature 412 (2001) 745–748.
[10] J.A. Ihalainen, S. D'Haene, N. Yeremenko, H. van Roon, A.A. Arteni, E.J. Boekema, R. van Grondelle, H.C.P. Matthijs, J.P. Dekker, Aggregates of the chlorophyll-binding protein IsiA (CP43′) dissipate energy in cyanobacteria, Biochemistry 44 (2005) 10846–10853.
[11] E.G. Andrizhiyevskaya, T.M. Schwabe, M. Germano, S. D'Haene, J. Kruip, R. van Grondelle, J.P. Dekker, Spectroscopic properties of PSI-IsiA supercomplexes from the cyanobacterium *Synechococcus* PCC 7942, Biochim. Biophys. Acta 1556 (2002) 265–272.
[12] N. Yeremenko, R. Kouril, J.A. Ihalainen, S. D'Haene, N. van Oosterwijk, E.G. Andrizhiyevskaya, W. Keegstra, H.L. Dekker, M. Hagemann, E.J. Boekema, H.C. Matthijs, J.P. Dekker, Supramolecular organization and dual function of the IsiA chlorophyll-binding protein in cyanobacteria, Biochemistry 43 (2004) 10308–10313.
[13] T.J. Ryan-Keogh, A.I. Macey, A.M. Cockshutt, C.M. Moore, T.S. Bibby, The cyanobacterial chlorophyll-binding-protein isia acts to increase the in vivo effective absorption cross-section of psi under iron limitation1, J. Phycol. 48 (2012) 145–154.
[14] E. Gantt, Phycobilisomes, Annu. Rev. Plant Physiol. 32 (1981) 327–347.
[15] M. Sarcina, C.W. Mullineaux, Mobility of the IsiA chlorophyll-binding protein in cyanobacterial thylakoid membranes, J. Biol. Chem. 279 (2004) 36514–36518.
[16] A.N. Melkozernov, T.S. Bibby, S. Lin, J. Barber, R.E. Blankenship, Time-resolved absorption and emission show that the CP43′ antenna ring of iron-stressed *Synechocystis* sp. PCC6803 is efficiently coupled to the photosystem I reaction center core, Biochemistry 42 (2003) 3893–3903.
[17] R. Berera, I.H.M. van Stokkum, J.T.M. Kennis, R. van Grondelle, J.P. Dekker, The light-harvesting function of carotenoids in the cyanobacterial stress-inducible IsiA complex, Chem. Phys. 373 (2010) 65–70.
[18] R. Berera, I.H.M. van Stokkum, S. d'Haene, J.T.M. Kennis, R. van Grondelle, J.P. Dekker, A mechanism of energy dissipation in cyanobacteria, Biophys. J. 96 (2009) 2261–2267.
[19] D.M. Niedzwiedzki, T. Tronina, H. Liu, H. Staleva, J. Komenda, R. Sobotka, R.E. Blankenship, T. Polivka, Carotenoid-induced non-photochemical quenching in the cyanobacterial chlorophyll synthase-HliC/D complex, BBA-Bioenegetics 1857 (2016) 1430–1439.
[20] H. Staleva, J. Komenda, M.K. Shukla, V. Slouf, R. Kana, T. Polivka, R. Sobotka, Mechanism of photoprotection in the cyanobacterial ancestor of plant antenna proteins, Nat. Chem. Biol. 11 (2015) 287–291.
[21] E.G. Andrizhiyevskaya, D. Frolov, R. van Grondelle, J.P. Dekker, Energy transfer and trapping in the photosystem I complex of *Synechococcus* PCC 7942 and in its supercomplex with IsiA, BBA-Bioenergetics 1656 (2004) 104–113.
[22] X. Feng, B. Neupane, K. Acharya, V. Zazubovich, R. Picorel, M. Seibert, R. Jankowiak, Spectroscopic study of the CP43′ complex and the PSI–CP43′ supercomplex of the cyanobacterium *Synechocystis* pcc 6803, J. Phys. Chem. B 115 (2011) 13339–13349.
[23] G.S. Orf, R.G. Saer, D.M. Niedzwiedzki, H. Zhang, C.L. McIntosh, J.W. Schultz, L.M. Mirica, R.E. Blankenship, Evidence for a cysteine-mediated mechanism of excitation energy regulation in a photosynthetic antenna complex, Proc. Natl. Acad. Sci. U. S. A. 113 (2016) E4486–E4493.
[24] S. Shcolnick, Y. Shaked, N. Keren, A role for mrgA, a DPS family protein, in the internal transport of Fe in the cyanobacterium *Synechocystis* sp. PCC6803, BBA-Bioenegetics 1767 (2007) 814–819.
[25] Y. Kashino, W.M. Lauber, J.A. Carroll, Q. Wang, J. Whitmarsh, K. Satoh, H.B. Pakrasi, Proteomic analysis of a highly active photosystem II preparation from the cyanobacterium *Synechocystis* sp. PCC 6803 reveals the presence of novel polypeptides, Biochemistry 41 (2002) 8004–8012.
[26] H. Kubota, I. Sakurai, K. Katayama, N. Mizusawa, S. Ohashi, M. Kobayashi, P. Zhang, E.-M. Aro, H. Wada, Purification and characterization of photosystem I complex from *Synechocystis* sp. PCC 6803 by expressing histidine-tagged subunits, BBA-Bioenegetics 1797 (2010) 98–105.
[27] D.M. Niedzwiedzki, J. Jiang, C.S. Lo, R.E. Blankenship, Low-temperature spectroscopic properties of the peridinin – chlorophyll *a* – protein (PCP) complex from the coral symbiotic dinoflagellate *Symbiodinium*, J. Phys. Chem. B 117 (2013) 11091–11099.
[28] P.L. Dilbeck, Q. Tang, D.J. Mothersole, E.C. Martin, C.N. Hunter, D.F. Bocian, D. Holten, D.M. Niedzwiedzki, Quenching capabilities of long-chain carotenoids in light harvesting-2 complexes from *Rhodobacter sphaeroides* with an engineered carotenoid synthesis pathway, J. Phys. Chem. B 120 (2016) 5429–5443.

[29] J.A. Greco, A.M. LaFountain, N. Kinashi, T. Shinada, K. Sakaguchi, S. Katsumura, N.C. Magdaong, D.M. Niedzwiedzki, R.R. Birge, H.A. Frank, Spectroscopic investigation of the carotenoid deoxyperidinin: direct observation of the forbidden $S_0 \rightarrow S_1$ transition, J. Phys. Chem. B 120 (2016) 2731–2744.
[30] I.H.M. van Stokkum, D.S. Larsen, R. van Grondelle, Global and target analysis of time-resolved spectra, BBA-Bioenergetics 1657 (2004) 82–104.
[31] M. Alfonso, G. Montoya, R. Cases, R. Rodriguez, R. Picorel, Core antenna complexes, Cp43 and Cp47, of higher-plant photosystem-II — spectral properties, pigment stoichiometry, and amino-acid-composition, Biochemistry 33 (1994) 10494–10500.
[32] T. Schulte, D.M. Niedzwiedzki, R.R. Birge, R.G. Hiller, T. Polivka, E. Hofmann, H.A. Frank, Identification of a single peridinin sensing Chl-*a* excitation in reconstituted PCP by crystallography and spectroscopy, Proc. Natl. Acad. Sci. U. S. A. 106 (2009) 20764–20769.
[33] J.L. Herek, M. Wendling, Z. He, T. Polivka, G. Garcia-Asua, R.J. Cogdell, C.N. Hunter, R. van Grondelle, V. Sundstrom, T. Pullerits, Ultrafast carotenoid band shifts: experiment and theory, J. Phys. Chem. B 108 (2004) 10398–10403.
[34] J.L. Herek, T. Polivka, T. Pullerits, G.J.S. Fowler, C.N. Hunter, V. Sundstrom, Ultrafast carotenoid band shifts probe structure and dynamics in photosynthetic antenna complexes, Biochemistry 37 (1998) 7057–7061.
[35] F. Ma, Y. Kimura, X.H. Zhao, Y.S. Wu, P. Wang, L.M. Fu, Z.Y. Wang, J.P. Zhang, Excitation dynamics of two spectral forms of the core complexes from photosynthetic bacterium *Thermochromatium tepidum*, Biophys. J. 95 (2008) 3349–3357.
[36] J.P. Zhang, H. Nagae, P. Qian, L. Limantara, R. Fujii, Y. Watanabe, Y. Koyama, Localized excitations on the B850a and B850b bacteriochlorophylls in the LH2 antenna complex from *Rhodospirillum molischianum* as probed by the shifts of the carotenoid absorption, J. Phys. Chem. B 105 (2001) 7312–7322.
[37] D.M. Niedzwiedzki, J.O. Sullivan, T. Polivka, R.R. Birge, H.A. Frank, Femtosecond time-resolved transient absorption spectroscopy of xanthophylls, J. Phys. Chem. B 110 (2006) 22872–22885.
[38] T. Polivka, C.A. Kerfeld, T. Pascher, V. Sundstrom, Spectroscopic properties of the carotenoid 3′-hydroxyechinenone in the orange carotenoid protein from the cyanobacterium *Arthrospira maxima*, Biochemistry 44 (2005) 3994–4003.
[39] Y. Zaushitsyn, K.G. Jespersen, L. Valkunas, V. Sundstrom, A. Yartsev, Ultrafast dynamics of singlet-singlet and singlet-triplet exciton annihilation in poly(3-2′-methoxy-5′-octylphenyl)thiophene films, Phys. Rev. B 75 (2007).
[40] H. Oh-Oka, S. Kamei, H. Matsubara, S. Lin, P.I. van Noort, R.E. Blankenship, Transient absorption spectroscopy of energy-transfer and trapping processes in the reaction center complex of *Chlorobium tepidum*, J. Phys. Chem. B 102 (1998) 8190–8195.
[41] S. Neerken, H.P. Permentier, C. Francke, T.J. Aartsma, J. Amesz, Excited states and trapping in reaction center complexes of the green sulfur bacterium *Prosthecochloris aestuarii*, Biochemistry 37 (1998) 10792–10797.
[42] G.N. He, D.M. Niedzwiedzki, G.S. Orf, H. Zhang, R.E. Blankenship, Dynamics of energy and electron transfer in the fmo-reaction center core complex from the phototrophic green sulfur bacterium *Chlorobaculum tepidum*, J. Phys. Chem. B 119 (2015) 8321–8329.
[43] D.M. Niedzwiedzki, R.E. Blankenship, Singlet and triplet excited state properties of natural chlorophylls and bacteriochlorophylls, Photosynth. Res. 106 (2010) 227–238.
[44] G.S. Orf, D.M. Niedzwiedzki, R.E. Blankenship, Intensity dependence of the excited state lifetimes and triplet conversion yield in the Fenna-Matthews-Olson antenna protein, J. Phys. Chem. B 118 (2014) 2058–2069.
[45] X.P. Wei, X.D. Su, P. Cao, X.Y. Liu, W.R. Chang, M. Li, X.Z. Zhang, Z.F. Liu, Structure of spinach photosystem II-LHCII supercomplex at 3.2 Å resolution, Nature 534 (2016) 69-+.
[46] T.M. Bricker, L.K. Frankel, The structure and function of CP47 and CP43 in photosystem II, Photosynth. Res. 72 (2002) 131–146.
[47] B. Loll, J. Kern, W. Saenger, A. Zouni, J. Biesiadka, Towards complete cofactor arrangement in the 3.0 Å resolution structure of photosystem II, Nature 438 (2005) 1040–1044.
[48] J. Nield, E.P. Morris, T.S. Bibby, J. Barber, Structural analysis of the photosystem I supercomplex of cyanobacteria induced by iron deficiency, Biochemistry 42 (2003) 3180–3188.